Check for updates

ChemPhysChem

Chemistry Europe
European Chemical Societies Publishing

Accepted Article

Title: Vibrational-Mode-Selective Modulation of Electronic Excitation

Authors: Jianxin Guan, Xinmao Li, Chengzhen Shen, Zhi Zi, Zhuowei Hou, Chuanqing Hao, Qirui Yu, Hong Jiang, Yuguo Ma, Zhihao Yu, and Junrong Zheng

This manuscript has been accepted after peer review and appears as an Accepted Article online prior to editing, proofing, and formal publication of the final Version of Record (VoR). The VoR will be published online in Early View as soon as possible and may be different to this Accepted Article as a result of editing. Readers should obtain the VoR from the journal website shown below when it is published to ensure accuracy of information. The authors are responsible for the content of this Accepted Article.

To be cited as: *ChemPhysChem* **2024**, e202400335

Link to VoR: https://doi.org/10.1002/cphc.202400335

WILEY VCH

10.1002/cphc.202400335

14397641, ja, Downloaded from https://chemistry-europe.onlinelibrary.wiley.com/doi/10.1002/cphc.202400335 by Peking University Health, Wiley Online Library on [01/06/2024]. See the Terms and Conditions (https://onlinelibrary.wiley.com/terms-and-conditions) on Wiley Online Library for rules of use; OA articles are governed by the applicable Creative Commons License

Accepted Manuscript

Vibrational-Mode-Selective Modulation of Electronic Excitation

Jianxin Guan[1†], Xinmao Li[1†], Chengzhen Shen[1†], Zhi Zi[1], Zhuowei Hou[1], Chuanqing Hao[1], Qirui Yu[1], Hong Jiang[1]*, Yuguo Ma[1]*, Zhihao Yu[1] and Junrong Zheng[1]*

[1]College of Chemistry and Molecular Engineering, Beijing National Laboratory for Molecular Sciences, Peking University, Beijing 100871, China

[†]These authors contributed equally to this work.

*Corresponding author. Email: junrong@pku.edu.cn (J.Z.); zhengjunrong@gmail.com; ygma@pku.edu.cn (Y.M.); jianghchem@pku.edu.cn (H. J.)

Jianxin Guan
College of Chemistry and Molecular Engineering
Peking University
292 Chengfu Road, Haidian District
Beijing, 100871, P. R. China
E-mail: guanjianxin1125@pku.edu.cn

Xinmao Li
College of Chemistry and Molecular Engineering
Peking University
292 Chengfu Road, Haidian District
Beijing, 100871, P. R. China
E-mail: lxm@stu.pku.edu.cn

Chengzhen Shen
College of Chemistry and Molecular Engineering
Peking University
292 Chengfu Road, Haidian District
Beijing, 100871, P. R. China
E-mail: shenchengzhen@pku.edu.cn

This article is protected by copyright. All rights reserved.

Zhi Zi
College of Chemistry and Molecular Engineering
Peking University
292 Chengfu Road, Haidian District
Beijing, 100871, P. R. China
E-mail: zhizi@pku.edu.cn

Zhuowei Hou
College of Chemistry and Molecular Engineering
Peking University
292 Chengfu Road, Haidian District
Beijing, 100871, P. R. China
E-mail: Houzw@pku.edu.cn

Chuanqing Hao
College of Chemistry and Molecular Engineering
Peking University
292 Chengfu Road, Haidian District
Beijing, 100871, P. R. China
E-mail: chuanqing.hao@pku.edu.cn

Qirui Yu
College of Chemistry and Molecular Engineering
Peking University
292 Chengfu Road, Haidian District
Beijing, 100871, P. R. China
E-mail: 1900011786@pku.edu.cn

Prof. Hong Jiang
College of Chemistry and Molecular Engineering
Peking University
292 Chengfu Road, Haidian District
Beijing, 100871, P. R. China
E-mail: jianghchem@pku.edu.cn

Prof. Yuguo Ma
College of Chemistry and Molecular Engineering
Peking University
292 Chengfu Road, Haidian District
Beijing, 100871, P. R. China
E-mail: ygma@pku.edu.cn

This article is protected by copyright. All rights reserved.

14397641, ja, Downloaded from https://chemistry-europe.onlinelibrary.wiley.com/doi/10.1002/cphc.202400335 by Peking University Health, Wiley Online Library on [01/06/2024]. See the Terms and Conditions (https://onlinelibrary.wiley.com/terms-and-conditions) on Wiley Online Library for rules of use; OA articles are governed by the applicable Creative Commons License

Accepted Manuscript

10.1002/cphc.202400335

Prof. Zhihao Yu
College of Chemistry and Molecular Engineering
Peking University
292 Chengfu Road, Haidian District
Beijing, 100871, P. R. China
E-mail: zhihaoyu@pku.edu.cn

Prof. Junrong Zheng
College of Chemistry and Molecular Engineering
Peking University
292 Chengfu Road, Haidian District
Beijing, 100871, P. R. China
E-mail: junrong@pku.edu.cn

This article is protected by copyright. All rights reserved.

14397641, ja, Downloaded from https://chemistry-europe.onlinelibrary.wiley.com/doi/10.1002/cphc.202400335 by Peking University Health, Wiley Online Library on [01/06/2024]. See the Terms and Conditions (https://onlinelibrary.wiley.com/terms-and-conditions) on Wiley Online Library for rules of use; OA articles are governed by the applicable Creative Commons License

Accepted Manuscript

14397641, ja, Downloaded from https://chemistry-europe.onlinelibrary.wiley.com/doi/10.1002/cphc.202400335 by Peking University Health, Wiley Online Library on [01/06/2024]. See the Terms and Conditions (https://onlinelibrary.wiley.com/terms-and-conditions) on Wiley Online Library for rules of use; OA articles are governed by the applicable Creative Commons License

Accepted Manuscript

Abstract

Vibrational-mode-selective modulation of electronic excitation is conducted with a synchronized femtosecond (fs) visible (vis) pulse and a picosecond (ps) infrared (IR) pulse. The mechanism of modulation of vibrational and vibronic relaxation behavior of excited state is investigated with ultrafast vis/IR, IR/IR, and vis-IR/IR transient spectroscopy, optical gating experiments and theoretical calculations. An organic molecule, 4'-(N,N-dimethylamino)-3-methoxyflavone (DMA3MHF) is chosen as the model system. Upon 1608 cm^{-1} excitation, the skeleton stretching vibration of DMA3MHF is energized, which can significantly change the shape of the absorption, facilitate the radiative decay and promote emission from vibrational excited states. As results, a remarkable enhancement and a slight blueshift in fluorescence are observed. The mode-selective modulation of electronic excitation is not limited in luminescence or photophysics. It is expected to be widely applicable in tuning many photochemical processes.

This article is protected by copyright. All rights reserved.

14397641, ja, Downloaded from https://chemistry-europe.onlinelibrary.wiley.com/doi/10.1002/cphc.202400335 by Peking University Health, Wiley Online Library on [01/06/2024]. See the Terms and Conditions (https://onlinelibrary.wiley.com/terms-and-conditions) on Wiley Online Library for rules of use; OA articles are governed by the applicable Creative Commons License

Accepted Manuscript

1. Introduction

Quantum coherences of electronic and nuclear motions may play important roles in photo-physical or -chemical processes in systems ranging from small molecules to macromolecules(*1-6*). The coupling of electronic and nuclear degrees of freedom, beyond the Born-Oppenheimer approximation, is critical in determining the outcomes of photochemical reactions(*7, 8*), the efficiency of emission(*9, 10*), and the rate and efficiency of electronic transitions(*11, 12*), which in turn provides a guidance for the modifications of relaxation behaviors of excited states(*13, 14*), excited state dynamics(*15, 16*), charge separation processes (*17*) and relaxation pathways(*18*).

It has been discovered that vibronic coherences as well as related energy redistributions play a vital role in many photo-induced processes such as isomerization, bond cleavage, electron transfer process and other chemical reactions (*6, 19-24*) of polyatomic molecules (*25*). The observations have inspired researchers to introduce specific vibrational excitations along particular reaction coordinates via ultrafast mid-IR pulses, to explore the effect of vibronic coupling in regulating molecular functions (*22, 26-28*). Previous approaches show that some electronic transition processes can be promoted or suppressed successfully(*29-35*). Modulations on many other ultrafast processes, e.g. singlet fission (SF) (*36-38*) and molecular luminescence processes (*25, 39, 40*), however, are not as effective.

Molecular fluorescence is one of the simplest but probably the most classical photophysical processes. Its efficiency is determined by the competition between radiative and nonradiative decays. If selective infrared excitations can modulate the

This article is protected by copyright. All rights reserved.

absorption of light and/or the evolution dynamics of electronic excited states, fluorescence can be tailored. Herein, we present a comprehensive investigation on the mechanism of mode-selective modulation of the vibronic relaxation processes with fluorescence as the spectator. In doing so, a picosecond (ps) IR pulse is frequency-tuned to be on resonance with molecular vibrations and a synchronized femtosecond (fs) visible pulse is subsequently applied to drive the molecule to its electronic excited state and the spontaneous emission is detected and analyzed.

2. Results and discussion

2.1 Fluorescence modulation with mode-selective IR excitations

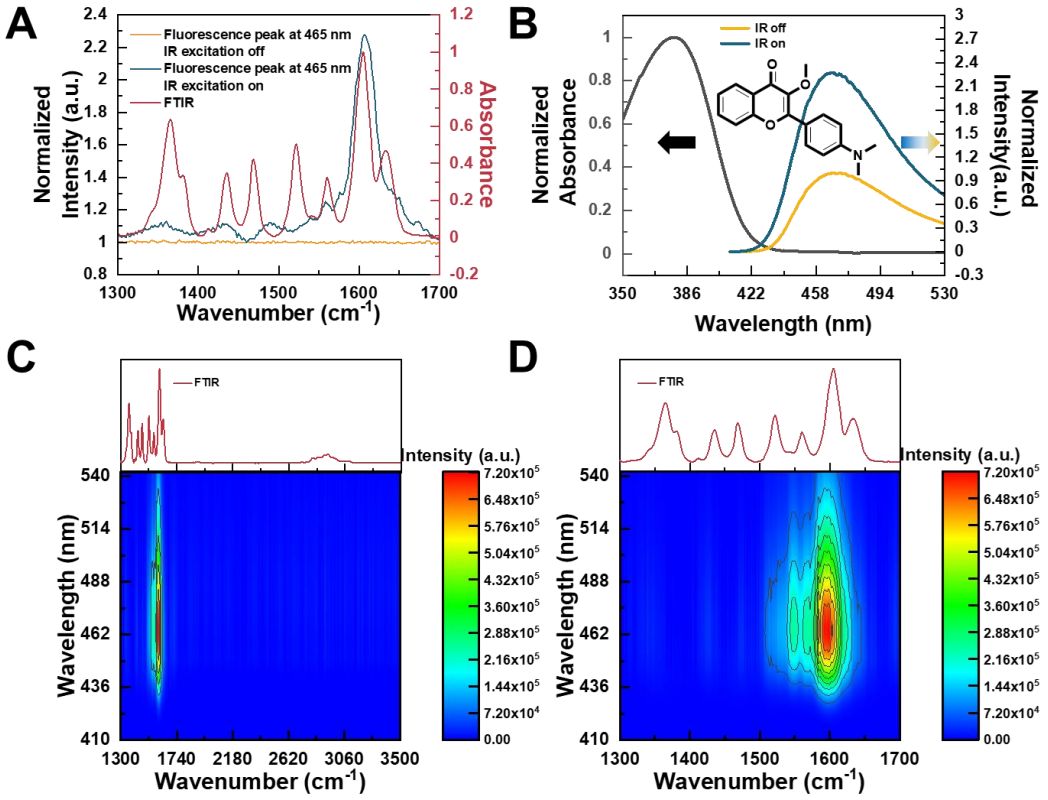

Fig. 1 Fluorescence modulations with mode-selective IR excitations. (A) Mode-selective fluorescence enhancement at the emission wavelength 465 nm in the infrared frequency range from 1300 cm^{-1} to 1700 cm^{-1} with visible excitation wavelength 450

This article is protected by copyright. All rights reserved.

14397641, ja, Downloaded from https://chemistry-europe.onlinelibrary.wiley.com/doi/10.1002/cphc.202400335 by Peking University Health, Wiley Online Library on [01/06/2024]. See the Terms and Conditions (https://onlinelibrary.wiley.com/terms-and-conditions) on Wiley Online Library for rules of use; OA articles are governed by the applicable Creative Commons License

Accepted Manuscript

14397641, ja, Downloaded from https://chemistry-europe.onlinelibrary.wiley.com/doi/10.1002/cphc.202400335 by Peking University Health, Wiley Online Library on [01/06/2024]. See the Terms and Conditions (https://onlinelibrary.wiley.com/terms-and-conditions) on Wiley Online Library for rules of use; OA articles are governed by the applicable Creative Commons License

Accepted Manuscript

nm of a 0.1 M DMA3MHF THF solution. The delay between IR and Vis pulses is 0 ps. **(B)** The UV-visible absorption spectrum of DMA3MHF in THF solution (black curve), and the fluorescence spectra excited with 450 nm light with and without IR excitation at 1608 cm^{-1}. Inserts are the molecular structures of DMA3MHF. The delay between IR and Vis pulses is also 0 ps. The fluorescence quantum yield is 46% excited at 380 nm. **(C)** Two dimensional fluorescence difference spectrum excited with 450 nm light with and without IR excitations at different frequencies. (D) Zoomed in spectrum of (C) in the range from 1300 cm^{-1} to 1700 cm^{-1}. Both C & D have been normalized with the power of IR laser. To avoid the influence of non-resonant excitation, The delay between IR and Vis pulses is 1.5 ps.

Fig.1 displays the mode-selective vibrational excitation dependence of fluorescence of a 4'-(N,N-dimethylamino)-3-methoxyflavone (DMA3MHF) dilution solution in 0.1 M THF of the vis-IR double and vis single resonance experiments. Upon excitation by 450 nm photons, DMA3MHF reaches the first electronic excited state and relaxes back to the ground state, emitting fluorescence peaked at 465 nm (apricot line in Fig.1 A & B, the noise of the apricot line in Fig.1A mainly comes from the excitation laser fluctuation and the detector noise). When a narrow-bandwidth picosecond infrared laser is on resonance with its vibrations, e.g. 1608 cm^{-1} which can energize the skeleton stretching vibrational mode, mode-selective fluorescence enhancements of more than two times are observed, illustrated as azure lines in Fig.1A&B. The enhancement is not only at a particular fluorescence wavelength, but also covering the entire spectrum

This article is protected by copyright. All rights reserved.

14397641, ja, Downloaded from https://chemistry-europe.onlinelibrary.wiley.com/doi/10.1002/cphc.202400335 by Peking University Health, Wiley Online Library on [01/06/2024]. See the Terms and Conditions (https://onlinelibrary.wiley.com/terms-and-conditions) on Wiley Online Library for rules of use; OA articles are governed by the applicable Creative Commons License

Accepted Manuscript

(Fig.1B). It is well known that high-frequency vibrations in room temperature liquids typically last only for a few picoseconds, whereas the fluorescence lifetime is at the time scale of a few to tens of nanoseconds. Therefore, the enhancement of fluorescence intensity by vibrational excitation displayed in fig.1A certainly not entirely due to the emission of the initial vibratory excited states. One of the main causes of enhanced fluorescence may be that vibrational excitation changes the shape of the absorption line, redshifting the absorption spectrum(*32, 34*), and thus excites more molecules. In order to distinguish these two roles, we measure the electronic absorptions and corresponding fluorescence spectra with and without infrared excitation. It is found that with the infrared excitation at 1608 cm^{-1}, the absorption doubles, and the fluorescence increases for 2.3 times. An extra 30% fluorescent enhancement compared to the absorption increase is found, indicating that the radiation rate is also increased.

The vibrational mode-selective fluorescence modulations are presented in Fig.1A. Ranging from 1300 cm^{-1} to 1500 cm^{-1}, where a series of rocking vibrations of benzene skeleton with different orientations reside, the effects are modest. A tremendous enhancement emerges at 1608 cm^{-1} which excites the skeleton stretching vibrations. Smaller enhancements are achieved with 1632 cm^{-1}, 1559 cm^{-1} photons that energizes the carbonyl stretch and rocking vibrations of benzene skeleton. Moreover, excitations of the C−H stretching vibrations located from 2700 to 3300 cm^{-1} have negligible effects, compared to other vibrational modes that are strongly coupled to skeletal motions (Fig.1 C & Fig. S11). It is conceivable that C−H stretching vibrations can barely change the structure of molecular skeleton which determines the extent of conjugation and the

This article is protected by copyright. All rights reserved.

14397641, ja, Downloaded from https://chemistry-europe.onlinelibrary.wiley.com/doi/10.1002/cphc.202400335 by Peking University Health, Wiley Online Library on [01/06/2024]. See the Terms and Conditions (https://onlinelibrary.wiley.com/terms-and-conditions) on Wiley Online Library for rules of use; OA articles are governed by the applicable Creative Commons License

Accepted Manuscript

electronic structures. Besides, the vibrational transition dipole moments of C−H stretching vibrations aren't aligned with (or even orthogonal to) that of the electronic transition dipole moment, which diminishes the vibration/electronic coupling.

The vibrational excitation at 1608 cm^{-1} leads to not only an intensity enhancement (Fig.1B), but also a blue-shift of emission peak, moving from 467.9 nm to 466.5 nm (Fig.S4), with the visible excitation at 450 nm. The blue-shift is not caused by subspecies that prefer to absorb at different wavelengths and emit differently, e.g. As displayed in Fig. S3, when the visible excitation wavelength shifts from 450 nm to 420 nm which is closer to the absorption center, the intensity of fluorescence increases tremendously, but the peak wavelength remains the same. The results imply that no subspecies that emit differently exist in the sample solution. It is interesting to note that when the IR pulse 5 ps ahead of the visible pulse, the enhancement of fluorescence intensity is reduced, and the peak blue-shift diminishes accordingly (Fig.S4).

This article is protected by copyright. All rights reserved.

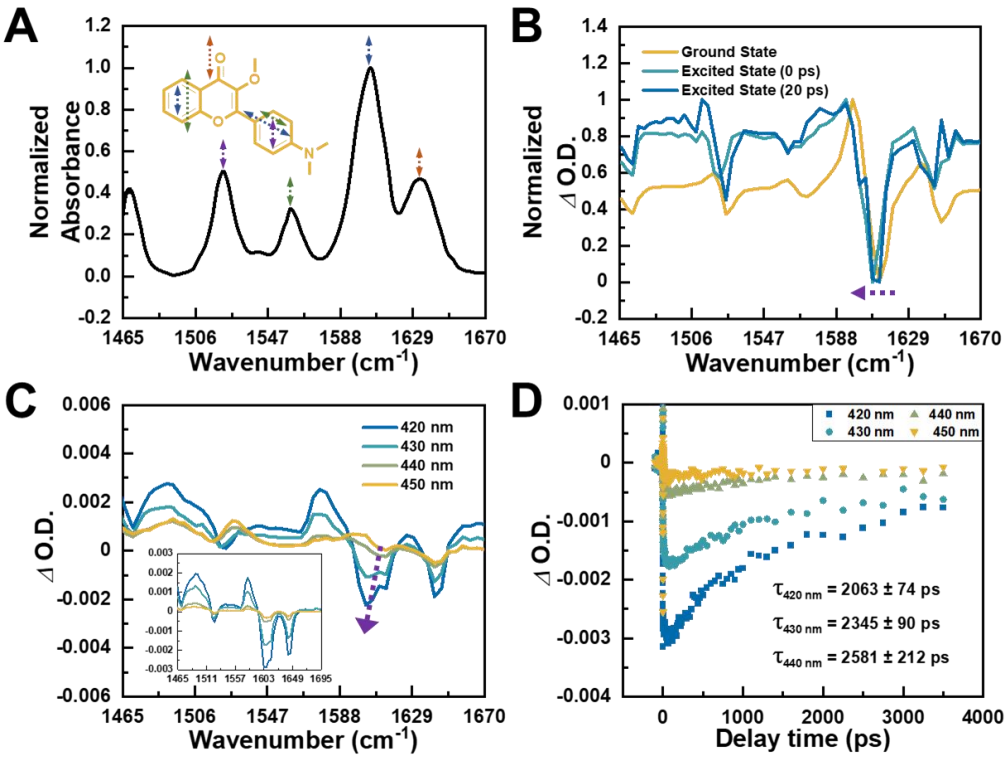

Fig. 2. (**A**) FTIR spectrum of DMA3MHF. Four different colored arrows illustrate the four different vibrational modes. (**B**) IR/IR and Vis-IR/IR transient spectra of DMA3MHF. The IR/IR spectrum is at time zero with excitation at 1610 cm^{-1}. The Vis-IR/IR spectra are collected with excitations at 450 nm and 1610 cm^{-1}. (**C**) Evolution of transient vibrational spectra of DMA3MHF with various visible excitations at the waiting time of 0.5 ps. The insert shows spectra at the waiting time of 100 ps. (**D**) Time dependent bleaching signals probed at about 1607 cm^{-1} with various visible excitations.

The fluorescence modulation mechanism by the vibrational excitations are further investigated with ultrafast IR/IR, Vis/IR and Vis/IR/IR spectroscopic techniques. Fig.2A displays the FTIR spectrum and peak assignments in the frequency range from 1465 to 1670 cm^{-1}. Results of visible (infrared) pump/infrared probe spectroscopy are illustrated in Fig.2B~D. The IR pump/IR probe spectrum at time zero with excitation

This article is protected by copyright. All rights reserved.

14397641, ja, Downloaded from https://chemistry-europe.onlinelibrary.wiley.com/doi/10.1002/cphc.202400335 by Peking University Health, Wiley Online Library on [01/06/2024]. See the Terms and Conditions (https://onlinelibrary.wiley.com/terms-and-conditions) on Wiley Online Library for rules of use; OA articles are governed by the applicable Creative Commons License

Accepted Manuscript

14397641, ja, Downloaded from https://chemistry-europe.onlinelibrary.wiley.com/doi/10.1002/cphc.202400335 by Peking University Health, Wiley Online Library on [01/06/2024]. See the Terms and Conditions (https://onlinelibrary.wiley.com/terms-and-conditions) on Wiley Online Library for rules of use; OA articles are governed by the applicable Creative Commons License

Accepted Manuscript

at 1610 cm^{-1} shows that the bleaching peak position is located at 1610 cm^{-1} (apricot in Fig.2B), the same as that in FTIR spectrum. With the additional electronic excitation at 450 nm, the bleaching peak redshifts ~ 4 cm^{-1} at time zero (both 450 nm and 1610 cm^{-1} pulses are temporally overlapped, and the delay between them and the probe IR pulse is also zero, Fig.2B). 20 ps after the visible and IR double excitation, the redshift disappears and the bleaching peak position recovers. The waiting time dependent peak shift is interesting and somewhat perplexing. It is likely caused by the combination of several factors. First, the peak appears at 1610 cm^{-1} is the overlap of the skeletal stretching vibration at frequency lower than 1610 cm^{-1} and the carbonyl stretching vibration at frequency higher than 1610 cm^{-1}. Second, the visible and IR double excitations send molecule to some vibrational excited states of the electronic excited state. Third, these vibrational states excited are expected to be strongly coupled to the electronic transition (otherwise they would not be excited when the electronic state is excited). Fourth, they are expected to be also coupled to the skeletal stretch through anharmonicity much stronger than the carbonyl stretch, as the skeletal stretch is more strongly coupled to the electronic transition as the fluorescence enhancement results suggest. Therefore, the excitations of the vibrations at the electronic excited state must shift the skeleton stretch out of its 0-1 transition frequency more than they do to the carbonyl stretch, resulting in a redshift of the overall bleaching peak observed in Fig.2B at time zero. However, once the excitations of these vibrations decay for a significantly amount, like after 20 ps, most of them go back to the ground state, and accordingly the redshift they cause diminishes. The explanation is further supported by Vis/IR

This article is protected by copyright. All rights reserved.

14397641, ja, Downloaded from https://chemistry-europe.onlinelibrary.wiley.com/doi/10.1002/cphc.202400335 by Peking University Health, Wiley Online Library on [01/06/2024]. See the Terms and Conditions (https://onlinelibrary.wiley.com/terms-and-conditions) on Wiley Online Library for rules of use; OA articles are governed by the applicable Creative Commons License

Accepted Manuscript

pump/probe data with visible excitation wavelength varying from 450 nm to 420 nm (Fig.2C). The bleaching peak red shifts from 1610 cm^{-1} with 450 nm excitation to 1602 cm^{-1} with 420 nm excitation, with the intensity increasing gradually. The intensity increases with a shorter excitation wavelength because 420 nm is closer to the absorption center than 450 nm. The bleaching peak redshift is probably because of the same reason discussed above. Upon 420 nm excitation, more and/or higher vibrations are excited at the electronic excited state, compared to 450 nm excitation, and therefore more skeletal stretches are shifted out of its 0-1 transition frequency, resulting in the overall peak redshift. Because the relaxations of these vibrations typically occur in a period of 80 fs ~8 ps (*41-45*), the redshift is gone once they go back to the vibrational ground state. As displayed in the insert of Fig.2C, after 100 ps, the bleaching peaks under different visible excitations go back to the same position as 450 nm. Fig.2D displays the waiting time dependent bleaching intensity under different visible excitations. It can be clearly seen that the decay is faster with a shorter excitation wavelength. The faster decay dynamics are caused by the relaxations of more vibrational excitations driven by a higher photonic energy (Fig.S17).

2.2 Time delay dependent Fluorescence enhancement

This article is protected by copyright. All rights reserved.

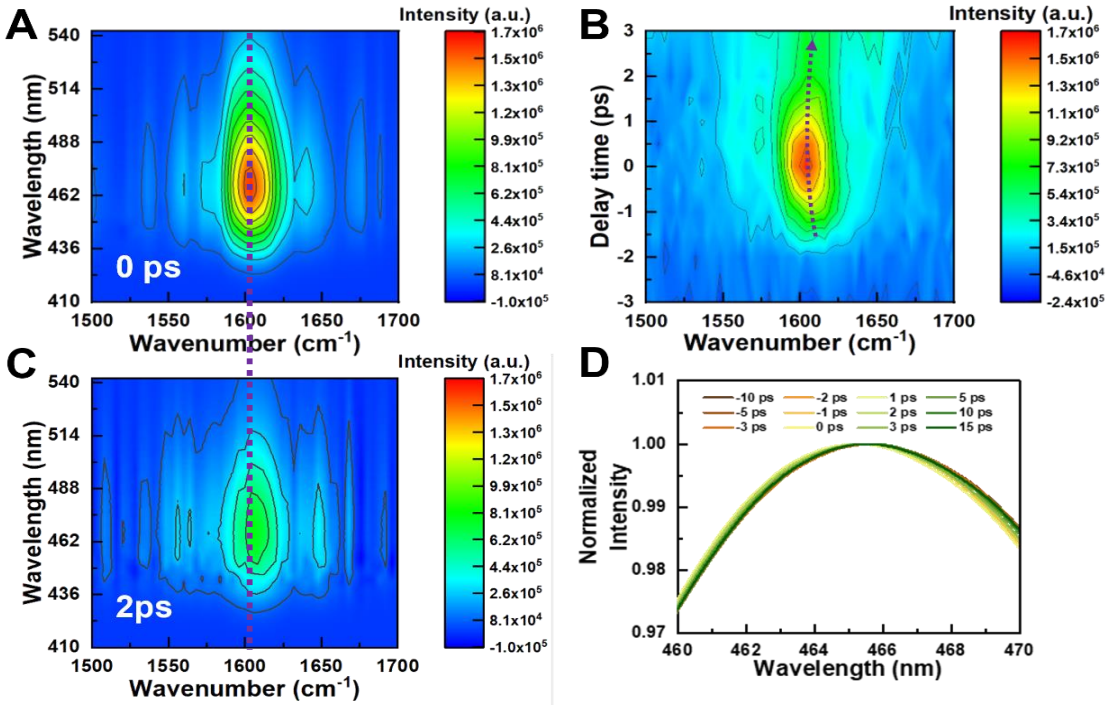

Fig. 3. (**A, C**) illustrate the evolution of infrared modulated fluorescence spectra: (A) the visible and IR pulses arriving at the sample simultaneously (0 ps) and (C) the IR pulse arriving 2 ps prior to the visible pulse. (**B**) Evolution of fluorescence intensity at 465 nm modulated with different vibrational excitations. **(D)** Normalized fluorescence emission spectra of DMA3MHF with different time delays between the visible and infrared laser pulses.

The fluorescence enhancement is dependent on the time interval between the two excitations. When the visible excitation proceeds prior to the IR excitation, the modulation effect illustrates a sharp growth from ~ 12% at -1.5 ps to ~230% at 0 ps (Fig.3B). Here, the negative time is defined as the visible pulse arrives at the sample prior to the IR pulse. The time zero is defined as the time point when the pump/probe signal reaches maximum. In contrast, the growth is apparently slower when the infrared excitation proceeds first (Fig.3B). Another time dependent feature is that the most

This article is protected by copyright. All rights reserved.

14397641, ja, Downloaded from https://chemistry-europe.onlinelibrary.wiley.com/doi/10.1002/cphc.202400335 by Peking University Health, Wiley Online Library on [01/06/2024]. See the Terms and Conditions (https://onlinelibrary.wiley.com/terms-and-conditions) on Wiley Online Library for rules of use; OA articles are governed by the applicable Creative Commons License

Accepted Manuscript

14397641, ja, Downloaded from https://chemistry-europe.onlinelibrary.wiley.com/doi/10.1002/cphc.202400335 by Peking University Health, Wiley Online Library on [01/06/2024]. See the Terms and Conditions (https://onlinelibrary.wiley.com/terms-and-conditions) on Wiley Online Library for rules of use; OA articles are governed by the applicable Creative Commons License

Accepted Manuscript

efficient modulation frequency of infrared laser shifts with the time interval, as illustrated by the dash arrow in Fig.3B. At time zero, it is 1608 cm^{-1}, and shifts to 1612 cm^{-1} at 3 ps. This shift can be observed by directly comparing spectra at time zero and 2 ps (Fig.3A&C). It is even more interesting that it also blue shifts in the negative time direction as the dash arrow indicates in Fig.3B.

Immediately after the visible excitation, the infrared laser interacts with molecules at the vibrational excited states of the electronic excited state. Both vibrational and electronic excited states red shift the IR-absorption. Long after the visible excitation (the negative time direction), the excited vibrations have relaxed, and the infrared laser interacts with molecules at the vibrational ground state of the electronic excited state. In this case, only the electronic excited state plays a role in redshifting the IR adsorption, the effect of which is only a portion of that at time zero. Therefore, the redshift amplitude becomes smaller (or appears blueshifting) along the negative time. On the contrary, at the positive time direction, after the infrared excitation, the visible pulse interacts with molecules at the vibrational excited state of the electronic ground state. In other words, the molecules that absorb IR photons are at the ground state, so the IR absorption frequency is higher than that at time zero when the molecules are excited, leading to the blueshift along the positive time. At the same time, the fluorescence blueshift also becomes smaller as the visible excitation is further away behind the IR excitation, as displayed in Fig.3D and discussed above.

2.2 Long life and initial fast decay of fluorescence enhancement

This article is protected by copyright. All rights reserved.

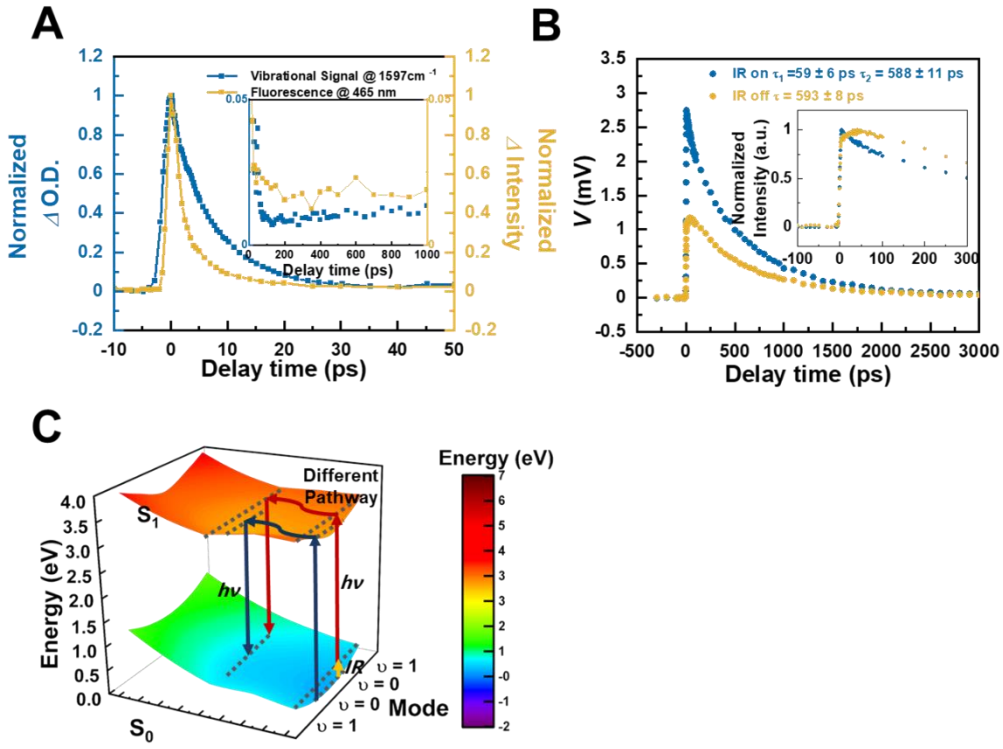

Fig. 4. (**A**) The evolution of fluorescence enhancement at 465 nm of DMA3MHF dependent on the time delay between the visible 450 nm excitation pulse and the IR 1608 cm^{-1} excitation pulse (apricot line)，and the vibrational decay signal excited with 1608 cm^{-1} and probed at 1597 cm^{-1} (azure line). The insert displays the signals at long delays. (**B**) Time dependent fluorescence intensity at 465 nm of DMA3MHF excited at 450 nm with and without 1608 cm^{-1} modulation. (**C**) Diagram illustrating the modulated radiative pathway that produces a blueshifted fluorescence.

Fig.4A displays the time dependent vibrational excitation signal excited at 1608 cm^{-1} and detected at 1597 cm^{-1} and the emission intensity at 465 nm of double excitations with 450 nm visible photons and 1608 cm^{-1} IR photons. In the initial 30 ps, the fluorescence decay is surprisingly faster than the vibrational decay. In Fig.4A, the

This article is protected by copyright. All rights reserved.

14397641, ja, Downloaded from https://chemistry-europe.onlinelibrary.wiley.com/doi/10.1002/cphc.202400335 by Peking University Health, Wiley Online Library on [01/06/2024]. See the Terms and Conditions (https://onlinelibrary.wiley.com/terms-and-conditions) on Wiley Online Library for rules of use; OA articles are governed by the applicable Creative Commons License

Accepted Manuscript

14397641, ja, Downloaded from https://chemistry-europe.onlinelibrary.wiley.com/doi/10.1002/cphc.202400335 by Peking University Health, Wiley Online Library on [01/06/2024]. See the Terms and Conditions (https://onlinelibrary.wiley.com/terms-and-conditions) on Wiley Online Library for rules of use; OA articles are governed by the applicable Creative Commons License

Accepted Manuscript

vibrational decay signal is rotation free, whereas in the double resonance experiments for fluorescence enhancement the polarization directions of the IR pulse and the visible pulse are parallel. Since the cross angle between the electronic and vibrational transition dipole moments is fixed, the molecular rotation during the time period between the two excitations can change the number of molecules that are doubly excited. Therefore, it is conceivable that the fluorescence enhancement decreases along with the randomization of molecular orientation, adding an additional signal decay channel besides the population decay. However, as displayed in SI (Fig.S15), the time dependent vibrational excitation signal with the parallel pump/probe polarization configuration is still significantly slower than the fluorescence decay in Fig.4A. The results indicate that the faster fluorescence dynamics must be caused by reasons other than molecular rotation. It is likely that in addition to the resonance vibrational absorption, the 1608 cm^{-1} IR pulse can also drive a nonresonant electronic response which can also increase the absorption of the 450 nm photon, resulting in a fluorescence enhancement. The nonresonant electronic response is expected to have a shorter lifetime than the skeleton stretch, and therefore the overall fluorescence decay in Fig.4A appears to be faster than the vibrational decay of the skeleton stretch. To test this hypothesis, the IR pulse is tuned to 2200 cm^{-1} where no vibrational peak resides, a fluorescence enhancement of about 25% is observed (Fig.S16 in SI), indicating that the IR pulse can indeed induce a nonresonant response to produce a sum frequency effect. The results also indicate a relatively large nonlinear response coefficient of DMA3MHF. This molecule actually has a structure that favors a large polarizability. It has an electron donating group – the

This article is protected by copyright. All rights reserved.

14397641, ja, Downloaded from https://chemistry-europe.onlinelibrary.wiley.com/doi/10.1002/cphc.202400335 by Peking University Health, Wiley Online Library on [01/06/2024]. See the Terms and Conditions (https://onlinelibrary.wiley.com/terms-and-conditions) on Wiley Online Library for rules of use; OA articles are governed by the applicable Creative Commons License

Accepted Manuscript

amine group on one side, and an electron pulling group – the carbonyl group on the other side. Electrons can be easily driven by electric field to move from one side to the other.

Interestingly, when the infrared laser interacts with the molecule before the visible pulse, a slight fluorescence enhancement can sustain for a very long period of time over 1 nanosecond (the insert in Fig.4A). Along with this observation, the vibrational signal also have a similar long tail (the insert in Fig.4A). The results indicate that probably long-lived low frequency modes populated by the relaxation of the skeleton stretch located at 1606 cm^{-1} can effectively enhance the fluorescence. The existence of the low frequency modes of which the lifetimes are comparable to that of fluorescence provides a channel for the observed fluorescence blueshift of the IR modulation discussed above. The emission can take place from these vibrational excited states of the electronic excited state, of which the wavelength is shorter than the regular fluorescence emitted from the vibrational ground state. Blueshifted fluorescence emitted from vibrational excited states of electronic excited has been previously investigated in several model systems such as Nile Blue and oxazine 1 (*46, 47*). Based on the fact of the slight fluorescence shift (about 1.5 nm) and theoretical analyses of vibrational modes, we tentatively assign the long-lived low-frequency vibrational modes to be the molecular wagging vibration located at about 86 cm^{-1} (Fig. S6B).

Optical gating experiments provide more insights into the modulation mechanism. As displayed in Fig.4B, besides the enhancement of luminescence, the time to reach emission maximum and the emission decay are also faster with 1608 cm^{-1} excitation.

This article is protected by copyright. All rights reserved.

14397641, ja, Downloaded from https://chemistry-europe.onlinelibrary.wiley.com/doi/10.1002/cphc.202400335 by Peking University Health, Wiley Online Library on [01/06/2024]. See the Terms and Conditions (https://onlinelibrary.wiley.com/terms-and-conditions) on Wiley Online Library for rules of use; OA articles are governed by the applicable Creative Commons License

Accepted Manuscript

With IR modulation, the molecular luminescence reaches maximum at ~4 ps，and decays with a fast component (59 ps) and a slow kinetics (588 ps). In contrast, the luminescence reaches maximum at ~ 40 ps and decays with a single exponential (593 ps) without IR modulation (Fig. 4B, Fig. S12 & Fig. S13). The results imply that the IR modulation facilitate the radiative decay rate and leads to more emissions from the vibrational excited states rather than the ground state. Both are consistent with the extra 30% fluorescence enhancement (over absorption increase) and blueshift discussed above.

Calculations on the electronic ground state and excited state are carried out to further explore the modulation mechanism. Density functional theory calculations are performed to obtain the equilibrium geometry and vibrational frequencies of molecule in both S0 and S1. The PBE0 in combination with 6-311++g (d, p) basis set is applied in all calculations. The dispersion correction and solvation models are also considered. The electronic structures of excited state S1 are calculated by TDDFT. The calculations are performed with the Gaussian 16 software (*48*). The calculated emission wavelength is 443.93 nm which is close to the experimental results. With the visible excitation wavelength and the electron transition dipole moment assumed to be constant, the absorption intensity is largely determined by the weighting of Franck-Condon factor. When the absorption wavelength is determined, the absorption strength of the molecule is different when it is under different vibration states. The calculation results show that nearly 50% more molecules can be excited with 1608 cm^{-1} than that excited with 1632 cm^{-1}, the carbonyl group stretching vibrational mode with 450 nm excitation, which is

This article is protected by copyright. All rights reserved.

agree with the experimental results. This also preliminarily indicates that our experiment can plot the coupling degree of S_0 and S_1 under different vibration modes. In addition, we use the Duschinsky rotation program to analyze the contribution of different vibration modes modulating the molecular conformational evolution from S_0 to S_1, and find that the excited skeleton vibration can facilitate the molecule to reach the energy minimum of S_1.

From the harmonic approximation we can obtain the instantaneous structure of the molecule as it vibrates and obtain Fig.4C which illustrates the emission from the vibrational excited state of the electronic excited state. After infrared excitation, the change of absorption spectrum results in the increase of absorbance and the excitation of more molecules, which is the main reason for the enhancement of fluorescence. On the other hand, the molecular evolution path to S_1opt is different by exciting different vibrational modes, and the skeleton vibration is the most efficient. At the same time, more molecules undergo radiation transition from high vibrational energy levels, resulting in fluorescence enhancement. More details can be found in the Supporting Information.

3. Concluding remarks

In summary, mode-selective vibrational excitations can effectively modulate the electronic transition and the evolution dynamics of the electronic excited state. Upon 1608 cm^{-1} excitation, the skeleton stretching vibration of DMA3MHF is energized, which can significantly increase the absorption intensity of the absorption edge, and facilitate the radiative decay and promote emission from vibrational excited states. As

This article is protected by copyright. All rights reserved.

14397641, ja, Downloaded from https://chemistry-europe.onlinelibrary.wiley.com/doi/10.1002/cphc.202400335 by Peking University Health, Wiley Online Library on [01/06/2024]. See the Terms and Conditions (https://onlinelibrary.wiley.com/terms-and-conditions) on Wiley Online Library for rules of use; OA articles are governed by the applicable Creative Commons License

Accepted Manuscript

14397641, ja, Downloaded from https://chemistry-europe.onlinelibrary.wiley.com/doi/10.1002/cphc.202400335 by Peking University Health, Wiley Online Library on [01/06/2024]. See the Terms and Conditions (https://onlinelibrary.wiley.com/terms-and-conditions) on Wiley Online Library for rules of use; OA articles are governed by the applicable Creative Commons License

Accepted Manuscript

results, a remarkable enhancement and a slight blueshift in fluorescence are observed. The mode-selective modulation of electronic excitation is not limited in luminescence or photophysics. It is expected to be widely applicable in tuning many photochemical processes.

Supplementary information is available in the online version of the paper.

Acknowledgements

This material is based upon work supported by the National Science Foundation of China (NSFC-22203006, 21927901, 92261206, 21627805, 12174012, 21673004, 21821004, 21674001 and 21790363), MOST (a special talent program) China, and the Beijing City. We also thank the support from the High-performance Computing Platform of Peking University for the computational resources.

Author contributions

J.Z. and J.G. designed experiments. J.Z. supervised the project. J.G., X.L. Z.H., and Z.Z. performed ultrafast experiments. J.G., X.L. and Y.M. prepared materials. J.G., X.L., Z.Y and J.Z. analyzed data. J.G., C.S., and H.J. conducted theoretical calculations. J.G., X.L., J.Z., Y.M., and H.J. prepared and revised the manuscript.

References:

1. A. H. Zewail, Femtochemistry: Atomic-Scale Dynamics of the Chemical Bond. *The Journal of Physical Chemistry A* **104**, 5660-5694 (2000).
2. M. M. Bishop *et al.*, Vibrationally Coherent Preparation of the Transition State for Photoisomerization of the Cyanine Dye Cy5 in Water. *J. Phys. Chem. B* **119**, 6905-6915 (2015).
3. R. W. Schoenlein, L. A. Peteanu, R. A. Mathies, C. V. Shank, The First Step in Vision: Femtosecond Isomerization of Rhodopsin. *Science* **254**, 412-415 (1991).
4. L. Zhu, J. T. Sage, P. M. Champion, Observation of Coherent Reaction Dynamics in Heme Proteins. *Science* **266**, 629-632 (1994).
5. A. Chenu, G. D. Scholes, Coherence in energy transfer and photosynthesis. *Annu. Rev. Phys. Chem.* **66**, 69-96 (2015).
6. M. Delor *et al.*, Directing the path of light-induced electron transfer at a molecular fork using

This article is protected by copyright. All rights reserved.

vibrational excitation. *Nat Chem* **9**, 1099-1104 (2017).

7. M. S. Schuurman, A. Stolow, Dynamics at Conical Intersections. *Annu. Rev. Phys. Chem.* **69**, 427-450 (2018).
8. W. Domcke, D. R. Yarkony, Role of conical intersections in molecular spectroscopy and photoinduced chemical dynamics. *Annu. Rev. Phys. Chem.* **63**, 325-352 (2012).
9. J. Guan, C. Shen, J. Peng, J. Zheng, What Leads to Aggregation-Induced Emission? *J Phys Chem Lett* **12**, 4218-4226 (2021).
10. J. Guan *et al.*, Direct Observation of Aggregation-Induced Emission Mechanism. *Angew. Chem. Int. Ed. Engl.*, (2020).
11. P. J. Johnson *et al.*, Local vibrational coherences drive the primary photochemistry of vision. *Nat Chem* **7**, 980-986 (2015).
12. G. Auböck, M. Chergui, Sub-50-fs photoinduced spin crossover in [Fe(bpy)3]2+. *Nature Chemistry* **7**, 629-633 (2015).
13. G. D. Scholes *et al.*, Using coherence to enhance function in chemical and biophysical systems. *Nature* **543**, 647-656 (2017).
14. M. Iwamura, S. Takeuchi, T. Tahara, Ultrafast excited-state dynamics of copper(I) complexes. *Acc. Chem. Res.* **48**, 782-791 (2015).
15. M. Olivucci, F. Santoro, Chemical selectivity through control of excited-state dynamics. *Angew. Chem. Int. Ed. Engl.* **47**, 6322-6325 (2008).
16. T. Elsaesser, W. Kaiser, Vibrational and Vibronic Relaxation of Large Polyatomic-Molecules in Liquids. *Annu. Rev. Phys. Chem.* **42**, 83-107 (1991).
17. J. D. Gaynor, J. Sandwisch, M. Khalil, Vibronic coherence evolution in multidimensional ultrafast photochemical processes. *Nature communications* **10**, (2019).
18. B. Lasorne, G. A. Worth, M. A. Robb, Excited-state dynamics. *Wiley Interdisciplinary Reviews: Computational Molecular Science* **1**, 460-475 (2011).
19. R. T. Hall, G. C. Pimentel, Isomerization of Nitrous Acid: An Infrared Photochemical Reaction. *The Journal of Chemical Physics* **38**, 1889-1897 (1963).
20. Q. Wang, R. W. Schoenlein, L. A. Peteanu, R. A. Mathies, C. V. Shank, Vibrationally coherent photochemistry in the femtosecond primary event of vision. *Science* **266**, 422-424 (1994).
21. A. Thomas *et al.*, Tilting a ground-state reactivity landscape by vibrational strong coupling. *Science* **363**, 615-619 (2019).
22. M. Delor *et al.*, Toward control of electron transfer in donor-acceptor molecules by bond-specific infrared excitation. *Science* **346**, 1492-1495 (2014).
23. A. M. Ronn, Infrared Laser Catalyzed Chemical Reactions. *Spectrosc. Lett.* **8**, 303-328 (1975).
24. B. C. Paulus, S. L. Adelman, L. L. Jamula, J. K. McCusker, Leveraging excited-state coherence for synthetic control of ultrafast dynamics. *Nature* **582**, 214-218 (2020).
25. T. Elsaesser, W. Kaiser, Vibrational and Vibronic Relaxation of Large Polyatomic Molecules in Liquids. *Annu. Rev. Phys. Chem.* **42**, 83-107 (1991).
26. Z. Lin *et al.*, Modulating unimolecular charge transfer by exciting bridge vibrations. *Journal of the American Chemical Society* **131**, 18060-18062 (2009).
27. A. A. Bakulin *et al.*, Mode-selective vibrational modulation of charge transport in organic electronic devices. *Nature communications* **6**, 7880 (2015).
28. M. Delor *et al.*, On the mechanism of vibrational control of light-induced charge transfer in donor-bridge-acceptor assemblies. *Nat Chem* **7**, 689-695 (2015).

This article is protected by copyright. All rights reserved.

14397641, ja, Downloaded from https://chemistry-europe.onlinelibrary.wiley.com/doi/10.1002/cphc.202400335 by Peking University Health, Wiley Online Library on [01/06/2024]. See the Terms and Conditions (https://onlinelibrary.wiley.com/terms-and-conditions) on Wiley Online Library for rules of use; OA articles are governed by the applicable Creative Commons License

Accepted Manuscript

29. H. Wang *et al.*, Bond-selective fluorescence imaging with single-molecule sensitivity. *Nat. Photonics*, 1-10 (2023).
30. L. Whaley-Mayda, A. Guha, S. B. Penwell, A. Tokmakoff, Fluorescence-Encoded Infrared Vibrational Spectroscopy with Single-Molecule Sensitivity. *J. Am. Chem. Soc.* **143**, 3060-3064 (2021).
31. L. Whaley-Mayda, S. B. Penwell, A. Tokmakoff, Fluorescence-Encoded Infrared Spectroscopy: Ultrafast Vibrational Spectroscopy on Small Ensembles of Molecules in Solution. *J. Phys. Chem. Lett.* **10**, 1967-1972 (2019).
32. J. von Cosel *et al.*, Vibrationally resolved electronic spectra including vibrational pre-excitation: Theory and application to VIPER spectroscopy. *J. Chem. Phys.* **147**, 164116 (2017).
33. L. J. G. W. van Wilderen, A. T. Messmer, J. Bredenbeck, Mixed IR/Vis Two-Dimensional Spectroscopy: Chemical Exchange beyond the Vibrational Lifetime and Sub-ensemble Selective Photochemistry. *Angew. Chem. Int. Ed.* **53**, 2667-2672 (2014).
34. M. Horz *et al.*, Vibrationally resolved two-photon electronic spectra including vibrational pre-excitation: Theory and application to VIPER spectroscopy with two-photon excitation. *J. Chem. Phys.* **158**, (2023).
35. D. Kern-Michler *et al.*, Controlling Photochemistry via Isotopomers and IR Pre-excitation. *J. Am. Chem. Soc.* **140**, 926-931 (2018).
36. H. Tamura, M. Huix-Rotllant, I. Burghardt, Y. Olivier, D. Beljonne, First-Principles Quantum Dynamics of Singlet Fission: Coherent versus Thermally Activated Mechanisms Governed by Molecular pi Stacking. *Physical review letters* **115**, 107401 (2015).
37. H. L. Stern *et al.*, Vibronically coherent ultrafast triplet-pair formation and subsequent thermally activated dissociation control efficient endothermic singlet fission. *Nat Chem* **9**, 1205-1212 (2017).
38. K. Miyata *et al.*, Coherent singlet fission activated by symmetry breaking. *Nat Chem* **9**, 983-989 (2017).
39. F. Laermer, T. Elsaesser, W. Kaiser, Ultrashort Vibronic and Thermal Relaxation of Dye Molecules after Femtosecond Ultraviolet Excitation. *Chem. Phys. Lett.* **156**, 381-386 (1989).
40. M. Baba *et al.*, Vibrational and rotational structure and excited-state dynamics of pyrene. *J. Chem. Phys.* **131**, 224318 (2009).
41. D. Ricard, W. H. Lowdermilk, J. Ducuing, Direct observation of vibrational relaxation of dye molecules in solution. *Chem. Phys. Lett.* **16**, 617-621 (1972).
42. D. Ricard, Vibrational relaxation in the first excited singlet state of rhodamine in solution. *The Journal of Chemical Physics* **63**, (1975).
43. A. J. Taylor, D. J. Erskine, C. L. Tang, Femtosecond vibrational relaxation of large organic molecules. *Chem. Phys. Lett.* **103**, 430-435 (1984).
44. M. J. Rosker, F. W. Wise, C. L. Tang, Femtosecond relaxation dynamics of large molecules. *Physical review letters* **57**, 321-324 (1986).
45. F. W. Wise, M. J. Rosker, C. L. Tang, Oscillatory Femtosecond Relaxation of Photoexcited Organic-Molecules. *J. Chem. Phys.* **86**, 2827-2832 (1987).
46. A. Mokhtari, J. Chesnoy, A. Laubereau, Femtosecond time- and frequency-resolved fluorescence spectroscopy of a dye molecule. *Chem. Phys. Lett.* **155**, 593-598 (1989).
47. A. Mokhtari, A. Chebira, J. Chesnoy, Subpicosecond fluorescence dynamics of dye molecules. *Journal of the Optical Society of America B* **7**, (1990).

This article is protected by copyright. All rights reserved.

14397641, ja, Downloaded from https://chemistry-europe.onlinelibrary.wiley.com/doi/10.1002/cphc.202400335 by Peking University Health, Wiley Online Library on [01/06/2024]. See the Terms and Conditions (https://onlinelibrary.wiley.com/terms-and-conditions) on Wiley Online Library for rules of use; OA articles are governed by the applicable Creative Commons License

Accepted Manuscript

10.1002/cphc.202400335

48. Frisch, M. J., et al., Gaussian 16 Rev. C.01, (2016).

This article is protected by copyright. All rights reserved.

14397641, ja, Downloaded from https://chemistry-europe.onlinelibrary.wiley.com/doi/10.1002/cphc.202400335 by Peking University Health, Wiley Online Library on [01/06/2024]. See the Terms and Conditions (https://onlinelibrary.wiley.com/terms-and-conditions) on Wiley Online Library for rules of use; OA articles are governed by the applicable Creative Commons License

Accepted Manuscript